Mechanical Engineering Projects Portfolio

Kweku Assou Joel SIKA- BS Mechanical Engineering

University of Illinois Urbana-Champaign

ksika2@illinois.edu

+1 (312) 972 6894

CONTENTS

INTRODUCTION & ABOUT ME

Introduction:

Welcome! I'm Joel SIKA, a senior undergraduate student studying Mechanical Engineering with a focus on manufacturing and systems control at the University of Illinois Urbana-Champaign. This portfolio offers a comprehensive overview of my mechanical engineering journey throughout my years as a student.

About me:

Despite the prevailing belief that childhood circumstances shape adulthood, my upbringing in Togo contradicts this notion. In a country with limited investment in research and technology, my exposure to engineering was minimal. However, Togo's educational system provided a strong foundation in mathematics and physics, igniting my passion for these subjects. Upon relocating to the United States, I encountered new intellectual and financial opportunities that reshaped my trajectory. Self-learning programming languages like C# and honing design skills in AutoCAD deepened my interest in engineering, leading me to pursue mechanical engineering. Financial independence enabled me to finance my education independently. Through coursework and projects, I gained comprehensive knowledge and experience in mechanical engineering disciplines, including design, analysis, manufacturing, and systems control.

SKATEBOARD BRAKING SYSTEM

Collaborated in a team of three to develop a product using a human-centered design approach. The project spanned 10 weeks, involving ideation, design, and analysis phases to create the final product.

Objective: To design a Skateboard braking system that allows efficient maneuverability in all weather conditions.

Steps of the design Process:

- Ideation and Sketch
- 3D-modeling
- Engineering drawings and Tolerance Analysis
- Manufacturing methods

SKATEBOARD BRAKING SYSTEM

Ideation and Sketch

The conception of any engineering product starts with ideation, in which various possible sketches of the product are established. As such, for this project, several conceptual ideas for the braking system were explored, and the most efficient one was selected based on manufacturability and engineering considerations. Therefore, the refined sketch of the braking system, as shown in the right image, was chosen due to its feasibility and engineering principle which relies on hydraulic force to provide stable control of the skateboard even in wintertime.

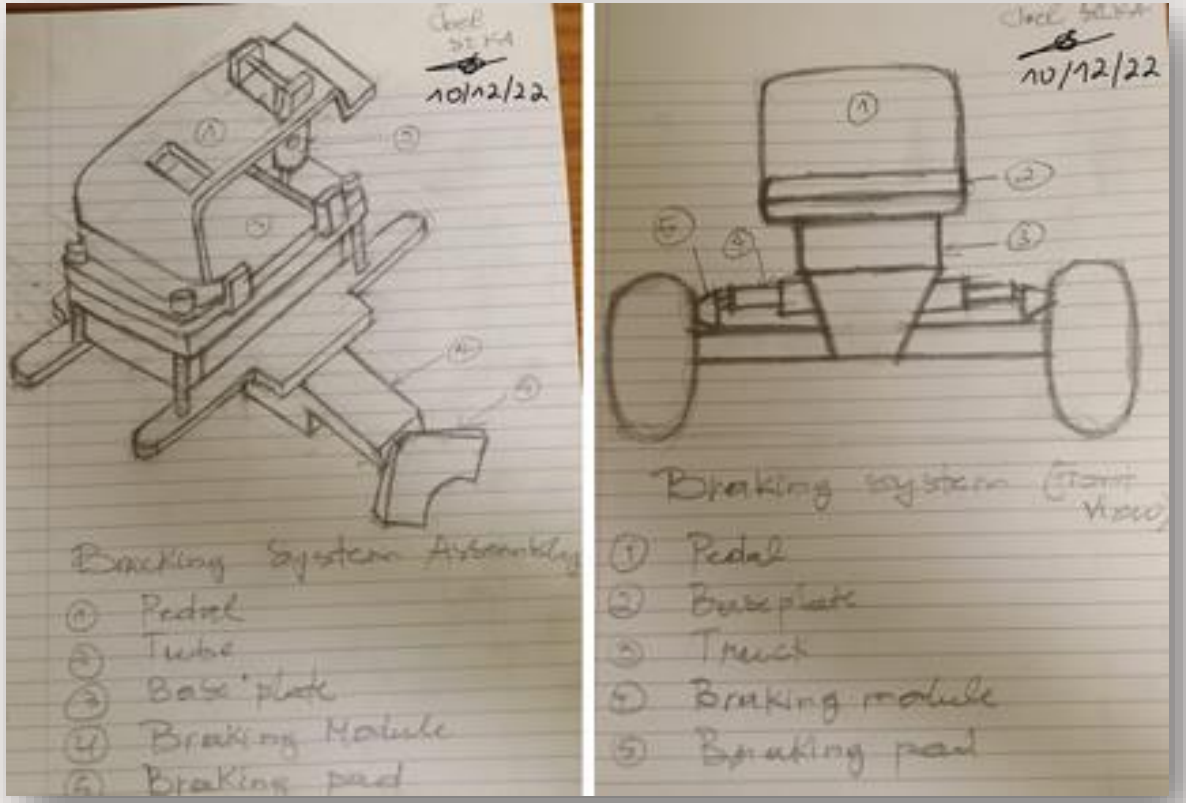

SKATEBOARD BRAKING SYSTEM

3D-Modeling

Following the ideation and sketch, a 3D model of the braking system is realized using Fusion 360. The braking system relies on hydraulic pressure to provide efficient maneuverability in harsh weather conditions. The system consists of three main components: a pedal, a piston, and a brake module. The pedal, which is made of aluminum sheet metal, operates like the system actuator. Indeed, by pressing on the pedal, enough force is provided to set the fluid inside the piston in motion. The hydraulic fluid passes through a set of tubes (not shown in the assembly) connecting the piston to the brake module. The buildup of pressure inside the brake module pushes the braking pad forward to interact with the skateboard wheels. As a result, a frictional force is developed between the braking pad and the skateboard wheels, forcing the skateboard to stop.

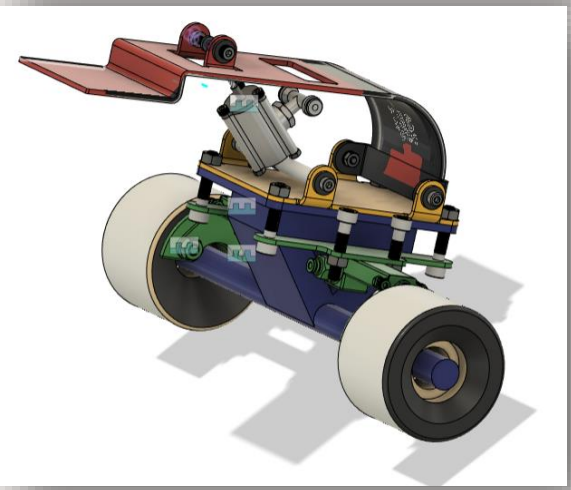

SKATEBOARD BRAKING SYSTEM

Engineering Drawings and Tolerance Analysis

When 3D-modeling a part, specifications must be taken to consider the manufacturability of the part. Those specifications are usually communicated through the engineering drawings of the part. Therefore, following the CAD model of the braking system components, several engineering drawings are generated to highlight the dimensions of the brake components. However, since it is impossible to accurately manufacture these components to their given dimensions, a tolerance analysis is performed to express the allowable range of variations in the brake component dimensions. For instance, in the bottom right image, a tolerance analysis is performed between four of the braking system components: a nylon bushing, a pedal, a base plate, and a screw shaft. This analysis reveals a clearance of 0.7 mm when the nylon bushing is fitted in either the baseplate or pedal hole, ensuring that the nylon bushing will always fit inside the baseplate or pedal hole under any manufacturing inaccuracy. The analysis further reveals an allowance of 0.01 mm and a fit of 0.372 mm between the nylon bushing hole and the screw shaft, confirming a clearance fit between those two components regardless of the dimensional inaccuracy yielded by manufacturing.

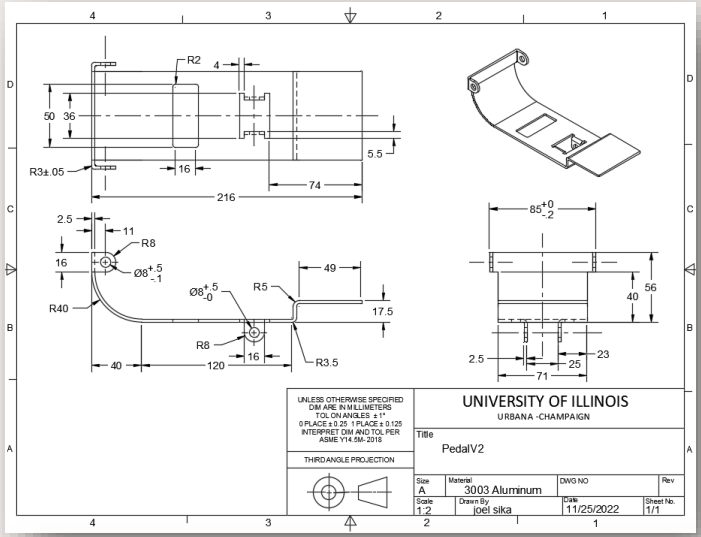

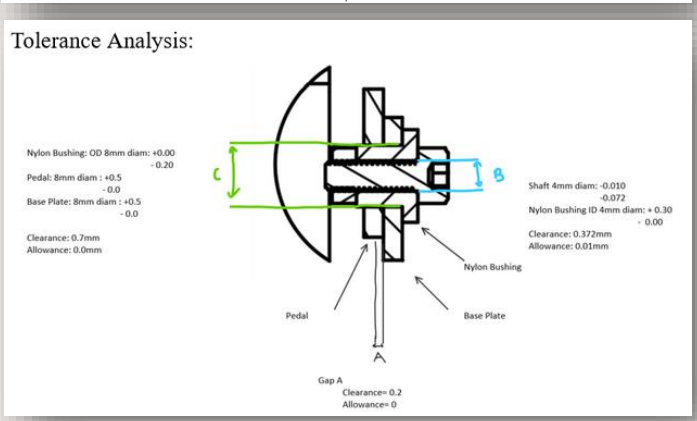

SKATEBOARD BRAKING SYSTEM

Manufacturing Methods

Most of the components of the skateboard braking system, except for screws and tubes, are not available on the market. Hence, there is a need to specify the manufacturing methods for these components. Three types of materials are used in the conception of the braking systems: aluminum sheet metal, rubber polymer, and aluminum metal. As such, the pedal and the baseplate, which are made of aluminum sheet metal, are manufactured using stamping and bending. Furthermore, the brake module body, which is made of aluminum, is manufactured using die casting. Additionally, the braking pad is manufactured using injection molding. The choice of these manufacturing methods is made considering cost and desired physical properties of the manufactured part.

Part #	Description	Material and Manufacturing Method (or order details if an off-the-shelf item)	Part Cost (fully burdened and catalog)	Quantity	Total Part Costs	Investment Costs (tooling, fixtures etc)
Part 1	Baseplate	Stamping and Bending (sheet metal): ANSI 3003	$1.14	1	$1.14	$15,979
Part 2	Braking Pad	Injection molding (rubber)	$0.04	1	$0.04	$5,365.16
Part 3	Brake Module Shaft	Molded Plastic - ABS : Injection molding - 4 cavity mold	$1.20	1	$1.20	$5,365
Part 4	Break Module Body	Aluminum Die Casting	$0.35	2	$0.70	$13,334.29
Part 5	Break Module Cap	Stamping and Bending Sheet Metal: ANSI 3003	$0.02	2	$0.04	$0.00
Part 6	Pedal	Stamping and Bending (sheet metal): ANSI 3003	$1.91	1	$1.91	$18,408.32
Part 7	Break Module Shaft Rubber Gaske	Roto & Blow Molding: SAN	$0.01	2	$0.02	$7,240.25
Part 8	Break Connector Plate	Stamping and Bending Sheet Metal: ANSI 3003	$0.08	2	$0.16	$0.00
Part 9	Piston Rubber Gasket	Roto & Blow Molding: SAN	$0.02	1	$0.02	$7,240.25
Part 10	Plastic Spacer	Sheet Plasic: ABS Extrusion Sheet GP	$0.11	2	$0.22	$2,604.65
Part 11	Piston Rod End	Bar and Tube Fab: ANSI 3003	$0.05	1	$0.05	$66.71
Part 12	Fine Thread Alloy Steel Socket Head Screw	Fine-Thread Alloy Steel Socket Head Screw	$0.10	16	$1.60	
Part 13	Aluminum Socket Head Screw	https://www.mcmaster.com/98511A741/	$0.10	2	$0.20	
Part 14	Aluminum Steel Socket Head Screw	https://www.mcmaster.com/91290A185/	$0.10	1	$0.10	
Part 15	Alloy Steel Socket Head Screw	https://www.mcmaster.com/91290A111/	0.0364	8	$0.29	
Part 16	Aluminum Hex Nut	https://www.mcmaster.com/91854A101/	$0.03	4	$0.12	
Part 17	Zinc-Plated Steel Hex Nut	https://www.mcmaster.com/90591A151/	$0.01	16	$0.17	
Part 18	Steel Hex Nut	https://www.mcmaster.com/90592A016/	$0.02	7	$0.12	
Part 19	Tube Connector	https://www.mcmaster.com/7699N45/	$0.94	1	$0.94	
Part 20	Tube	https://www.mcmaster.com/7397N12/	$0.93	2	$1.86	
Part 21	Main Piston Body	Stage Tooling (Sheet Metal): ANSI 3003	$0.21	1	$0.21	$18,027.00
Part 22	Piston Cap	Waterjet/Bend (Sheet Metal): ANSI 3003	$0.05	1	$0.05	
				TOTALS	$11.16	$93,631

AUTOMATED CHOPPER

Automated chopper is the first hands-on oriented project that I did in my mechanical engineering design class. The project highlights the design and analysis of mechanical machine components.

Objective: To create a machine that cut vegetables without human interference.

Module of the project:

- Ideation and CAD modeling
- Mechanism components
- Manufacturing
- Position-Velocity-Acceleration (PVA) analysis

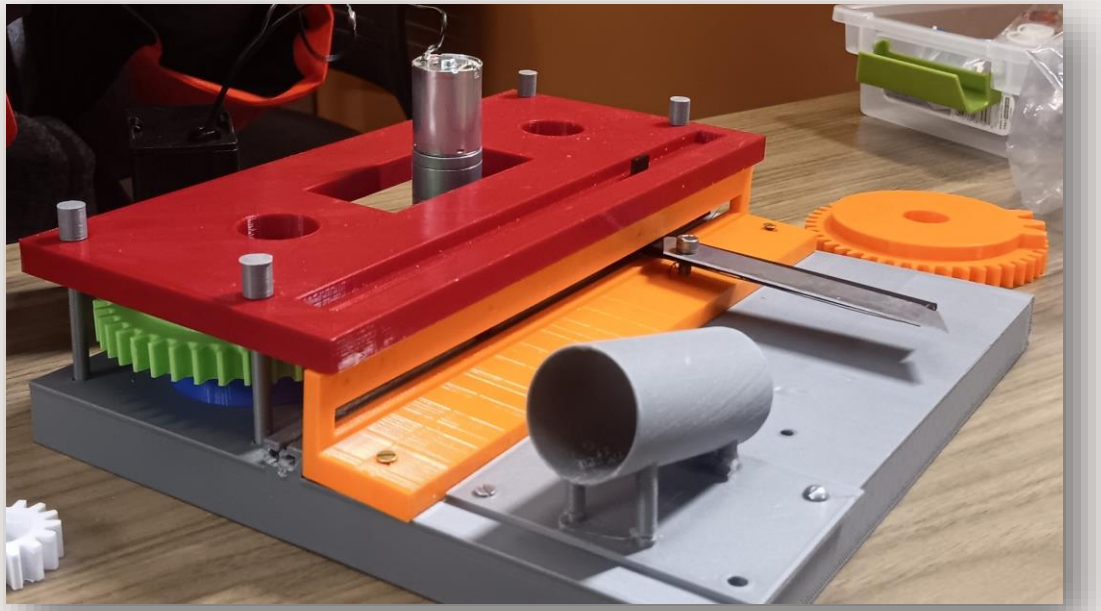

AUTOMATED CHOPPER

Ideation and 3D-Modeling

Given the objective of the project, it is needed to create a machine that incorporates both return and feeding mechanisms. Those two mechanisms enable the machine to operate without human interference. The return mechanism is constructed using a chassis, four gears, and one gear rack. These four gears include two output gears, an input gear and an idle gear. The feeding mechanism, on the other hand, was implemented using a gravity-based holder that carries vegetables during slicing. Hence, by motorizing the input gear, the two output gears rotate in opposite direction. This antagonist motion of the output gears enable the gear rack to vertically slide forward and backward and cut vegetables held by the feeding mechanism.

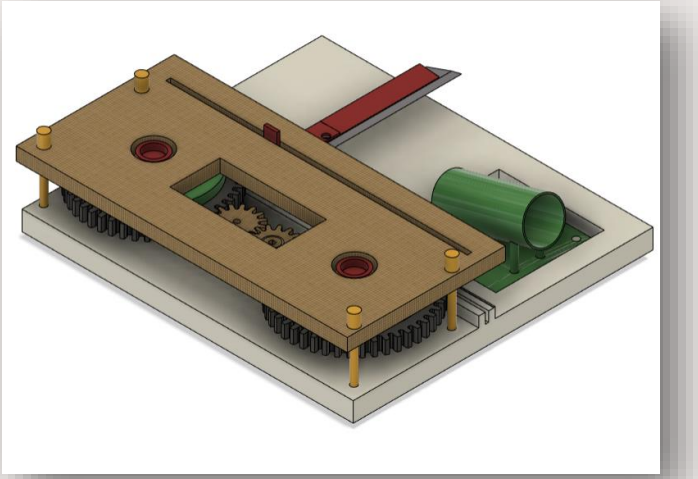

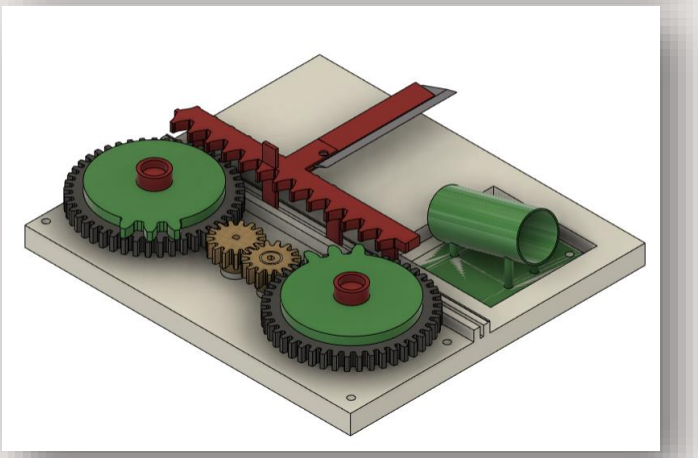

AUTOMATED CHOPPER

Mechanism Components:

- **Chassis**

The chassis , as shown in the top right CAD model, is designed to support the four gears, the gear rack and the holder. As such, it encompasses four protrusions for the gears, a slider constraint for the gear rack and a cut for the holder.

- **Input and Idle gears**

The bottom right CAD model shows the design of the input and idle gears. The input gears, which is motorized in the mechanism, is designed using a 3:1 gear ratio (with respect to the output gears) to derive enough torque from the motor. The idle gear, although not included in the gear ratio, is the main component creating the returning mechanism. Indeed, it is designed to allow the two output gears to rotate in opposite direction.

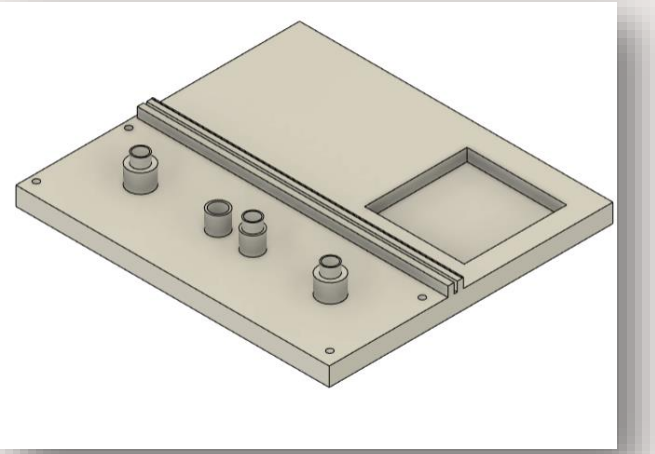

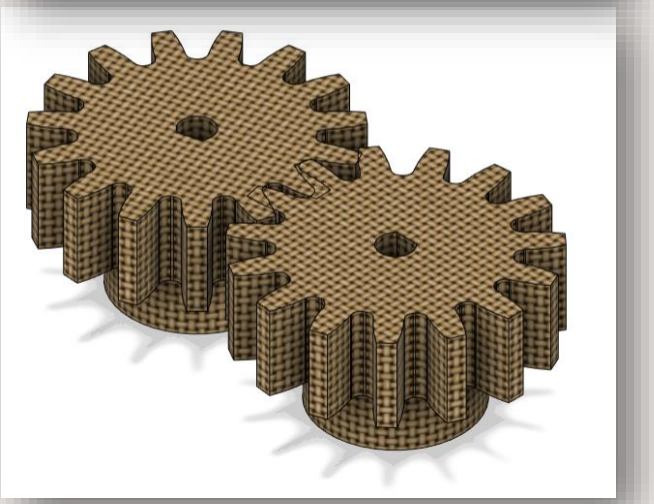

AUTOMATED CHOPPER

Mechanism Components:

- **Output Gears**

The two output gears are shown in the top right CAD model. They serve two purposes. First, they are designed using a gear ratio that allow them to rotate slower than the motor; thereby providing sufficient mechanical force to cut vegetables. Additionally, they rotate in opposite direction which enables the gear rack to slide upward and downward.

- **Gear rack and steel blade**

The bottom right CAD model shows the gear rack and the blade. The gear rack is coupled to the two output gears. Therefore, as these latter rotate, they allow the gear rack to move up and down inside the slider constraint of the chassis. As the gear rack is moving, it drives the steel blade which then cut vegetables.

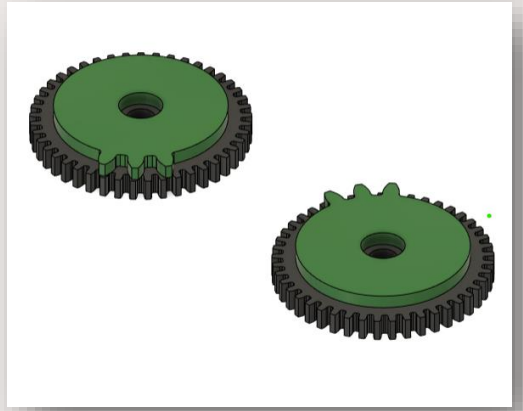

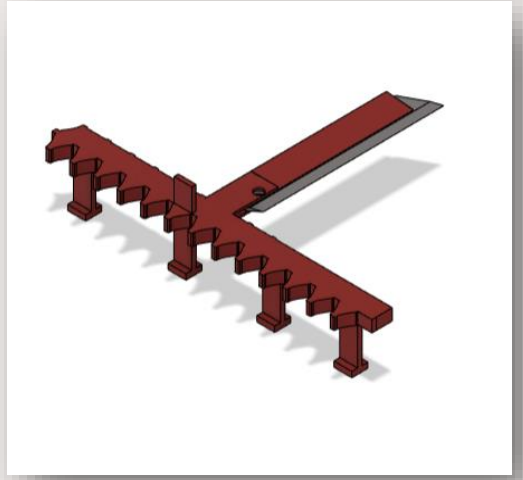

AUTOMATED CHOPPER

Mechanism Components:

- **Holder**

The top right CAD model displays the holder. The holder represents the gravity-based feeding mechanism. It encompasses a hollow cylinder that is titled to not only hold vegetables during cutting but also allow them to slide after cutting.

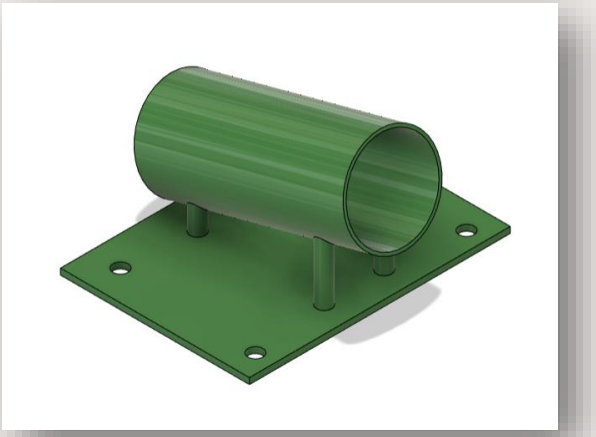

- **Coverplate**

The coverplate is shown in the bottom right CAD model. It includes two circular hole for the two output gears bushing, a rectangular hole for the motor and an additional vertical slider constraint for the gear rack. Furthermore, the coverplate acts as a constraint for the two output gears. Indeed, the rotational motion of the output gears results in an upward force which tends to unbalance the output gears. Having the coverplate, therefore, nullify the unbalanced forced.

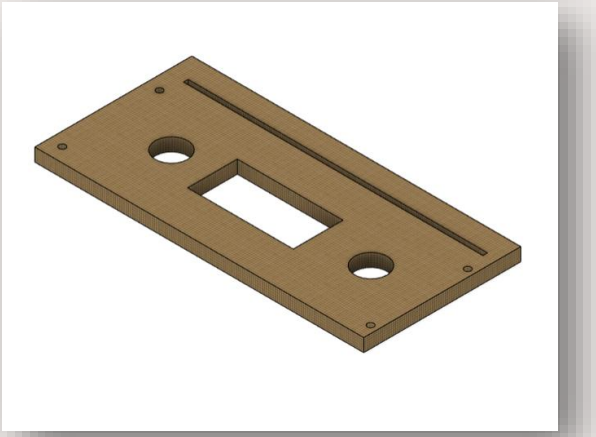

AUTOMATED CHOPPER

Manufacturing

The manufacturing process used in this project is 3D-printing. As such, the CAD model of the components are converted into STL files using Fusion 360. Next, these files are imported in Ultimaker Cura where the STL files are sliced into layers for printing.

Position-Velocity-Acceleration

The purpose of PVA analysis is to keep track of position and velocity of some of the mechanism components using a set of vector loop equations. For this analysis, the four gears and the gear rack are modeled as linkages. Then, using MATLAB, the mechanism is stimulated, and the gear rack position is plotted as function of the angular position of the input gear. The plot reveals a sinusoidal relationship between the gear rack and the input gear which effectively align with the upward and downward planar motion of the gear rack.

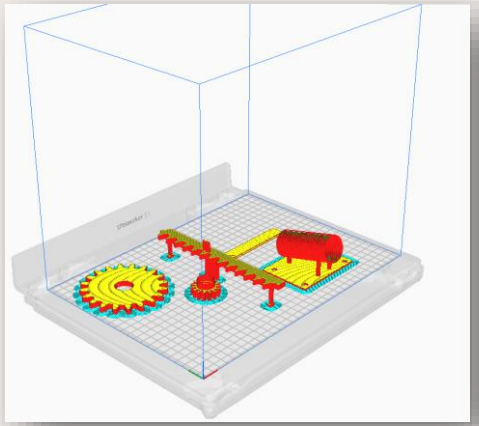

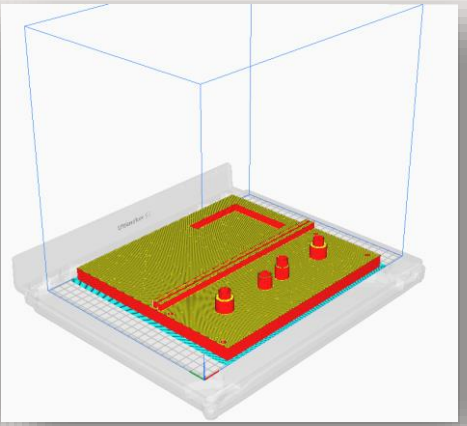

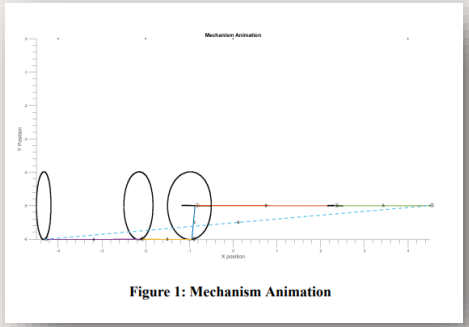

Figure 1: Mechanism Animation

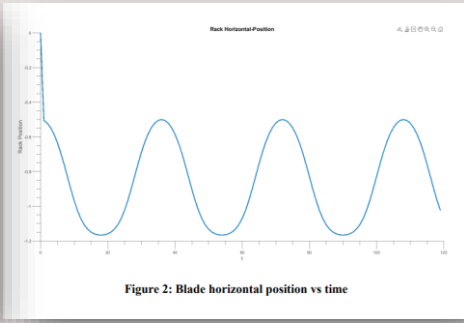

Figure 2: Blade horizontal position vs time

HEAT TRANSFER INDEPENDENT STUDY

Abstract

This study purports to investigate the effect of thermal contact surface resistance on heat flux. No surface is smooth. Therefore, when two non-smooth surfaces are in contact, there is a gap from which heat transfer may occur either through radiation, convection or conduction. This latter is the principal mode of heat transfer of interest in this study. In the investigation, cylindrical samples of brass are sanded using sandpaper of 120 and 150 grit size. By superposing each two of the samples in a hollow insulation foam and heating the exposed surface of the bottom sample, it is noticeable that the heat flux varies depending on the roughness at the contact surface. Indeed, samples that are sanded using 150 grit size sandpaper have less thermal surface resistance than those sanded at 120 grit size. This observation confirms that thermal surface resistance impedes heat flux. The higher the thermal surface resistance at the contact of two materials, the lower the heat flux conducted between these two materials.

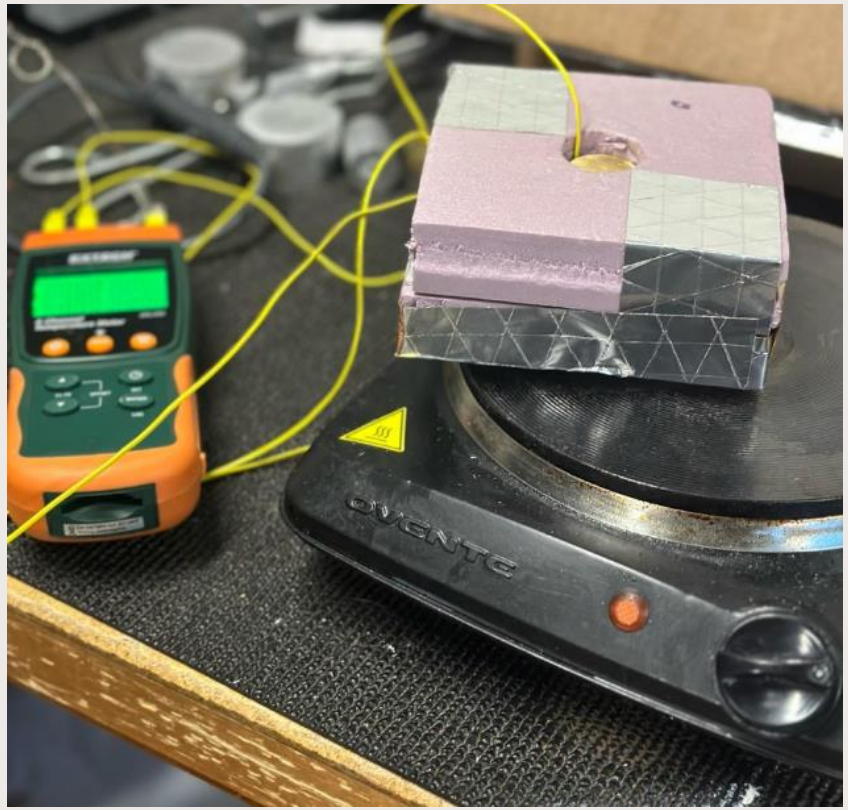

HEAT TRANSFER INDEPENDENT STUDY

Introduction

Thermal contact resistance is a phenomenon in which heat flow is impeded at the contact interface of two materials. Understanding thermal contact resistance is a critical issue in the efficient discharge of the heat waste of electronics, and large-scale integrated circuits. For this study, particular attention is given to thermal contact resistance effect on conduction heat flux under steady state conditions. To highlight the effect of thermal contact resistance, cylindrical blocks of brass with known thickness and thermal conductivity but difference surface roughness are used. Furthermore, these samples are placed in a hollow insulation foam to ensure that the heat transfer at the contact surface is solely by conduction and to avoid radial, and azimuthal variations of temperature. Additionally, in the laboratory experiment, three temperature measurements T_1, T_2, T_3 are taken using thermocouples. Under steady state condition ,no internal energy generation ,and one-dimensional flow, the heat equation ($\nabla q + \delta = \rho c \frac{dT}{dt}$), yields $q = \frac{\Delta T}{\frac{L}{k}}$. Therefore, the heat flux through the samples is calculated using :

$$q = \frac{\Delta T}{\frac{L_1}{k_1} + \frac{L_2}{k_2} + RA} \text{ or } q = \frac{T_3 - T_2}{\frac{L_2}{k_2}}$$

HEAT TRANSFER INDEPENDENT STUDY

Experimental Procedure

The experiment is conducted using three cylindrical blocks of brass. One sample of brass , denoted brass A, is sanded at one side using 120 grit size sandpaper. A second sample of brass, denoted brass B, is sanded using 150 grit size sandpaper. The third sample of brass, denoted brass C, is left un-sanded and is assumed to have an ideal smooth surface. Brass A and C are stacked with the smooth surface of brass C in contact with Brass C surface. Then, three thermocouples is placed at the exposed surface of brass A, brass C, and the contact surface of Brass A and C. The set-up is then placed on a hot plate which is configured to maintain a constant temperature. Three temperature readings T_1, T_2, T_3 are then taken as soon as steady state is reached. T_1 is the temperature at the contact surface of the sample and the hot plate. T_2 is the temperature at the contact surface between the stacked samples and T_3 is the temperature at the exposed surface of the top sample. Finally, three other cases are performed stacking Brass C on top of the sanded surface of Brass A, Brass C on top of the sanded surface of brass B and sanded surface of Brass A in contact with sanded surface of brass B, respectively.

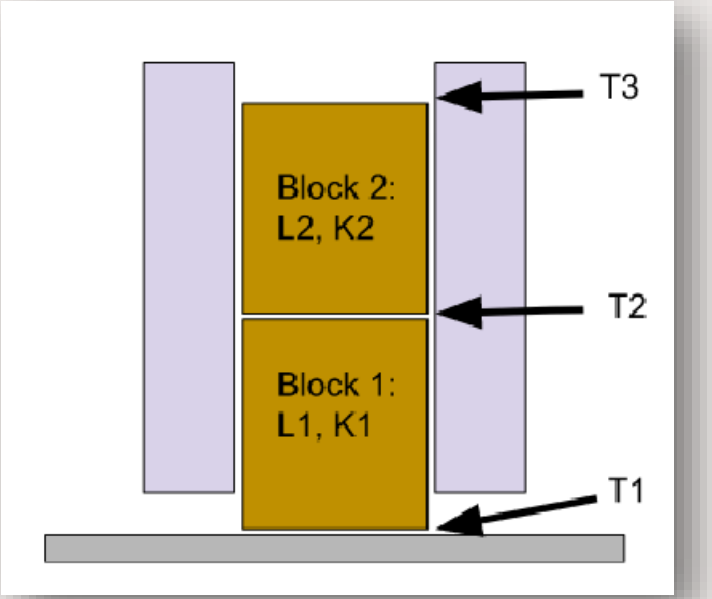

HEAT TRANSFER INDEPENDENT STUDY

Results

The data collected during the laboratory experiment shows that as the thermal contact resistance between two surfaces increases, the heat flux conducted decreases. This suggests that heat flux is inversely proportional to the thermal contact resistance. Furthermore, the samples sanded using 150 grit size present less resistance to heat flux than the samples sanded using 120 grit size. In applications ,involving thermal contact resistance, where heat flux needs to be maximized, several options can be taken to reduce thermal surface contact resistance. Indeed, thermal contact resistance at the interface can be reduced by applying a large force normal to the interface to flatten irregularities. Alternatively, applying a non-Newtonian fluid suspension , like a paste, between the interfaces of the solids layer significantly increases the heat flux.

System identification, PID and Lead Compensator Design for XY stage

The XY stage, located in the Grainger College of Engineering Hydraulic Lab, is a two-dimensional moving platform comprising X and Y axes. Each axis is powered by a brushless motor. The Y-stage motor is linked to a gear reduction system and then a belt for motion, while the X-stage motor is connected to a gear reduction system and leadscrew for motion generation.

Objective: Identify the transfer functions of XY-stage. Using these transfer functions, design a PID controller to follow a desired trajectory. Finally, design a lead controller to guarantee robustness of the moving stage.

Module:

- Closed-loop system identification
- PID control with trajectory generation
- Lead compensator design

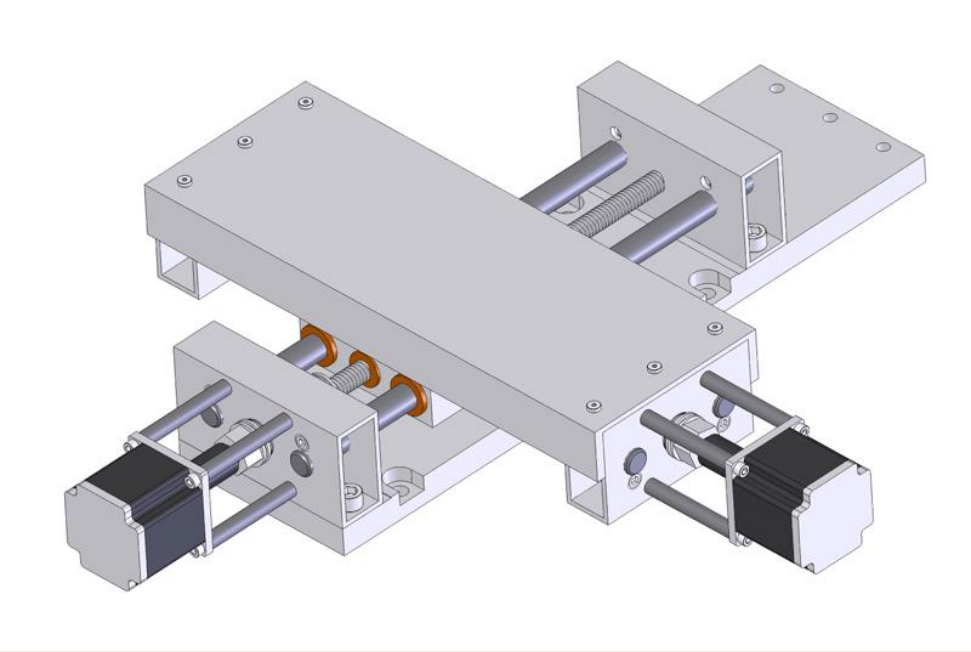

System identification, PID and Lead Compensator Design for XY stage

Closed-Loop System Identification

For the identification of the XY stage, each plant transfer function takes the form $\frac{K_{sys}}{s*(\tau_{sys}*s+1)}$. Considering this transfer function, it is evident that an open-loop is not useful for identifying the system, as it only allows the stage to move until the it reaches its limit. On the contrary, closing the loop with a proportional gain K_p not only enables the stage to move within its limit ,but also yields a second order transfer function of the form $\frac{w_n^2}{s^2+2\zeta w_n s+w_n^2}$ that can be employed to identify the plant transfer function.

Hence, using MATLAB Simulink, the closed-loop unity feedback system is constructed for each axis of the stage. The physical plant is stimulated using a signal block generator with a 5 mm amplitude square wave at a frequency of 0.25 Hz.

The lower right picture shows the ramp response plot of the physical plant over several periods. From the response of the system over one period, the natural frequency and the damping ratio of the closed system is determined. Based on the value of these two parameter, the X and Y stage transfer functions are respectively identified as follows:

$$G_x = \frac{350}{s*(0.046*s+1)}$$

$$G_y = \frac{475}{s*(0.051*s+1)}$$

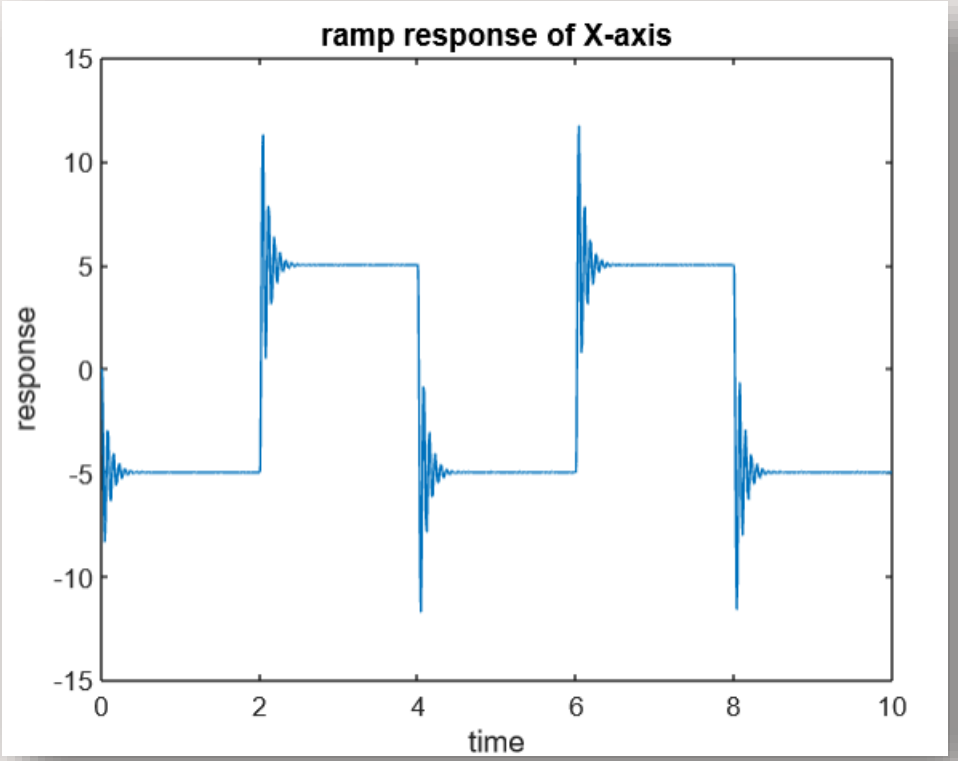

System identification, PID and Lead Compensator Design for XY stage

Proportional-Integral-Derivative (PID) control of the XY stage

The closed-loop system identification enabled us to derive the mathematical models for each axis of the XY stage. Specifically, the x-axis is described by $G_x = \frac{350}{s*(0.046*s+1)}$, and the y-axis is governed by $G_y = \frac{475}{s*(0.051*s+1)}$. Using these models, a controller can be designed to guide the plant's behavior in response to an input signal.

The controller of interest in this case is a PID controller, which controller has the mathematical form $\mathrm{k}_p + \mathrm{k}_i * \frac{1}{\mathrm{s}} + \mathrm{k}_d * \mathrm{s}$. Tuning the k_p, k_i, and k_d parameters of the controller involves exciting the system with a unit step input. However, the final signal input to the physical plant is a smooth transitioning sinusoidal signal, allowing the XY stage to follow a circular trajectory in such a way that if a pen were attached to the stage, it would draw a circle.

Moreover, as the derivative term "s" is impractical to implement, an approximate derivative transfer function, $\frac{500*s}{s+500}$, proven to be adequate for the physical plant, is used.

The accompanying pictures on right illustrate the closed-loop block diagram for the stage x-axis and y-axis, respectively.

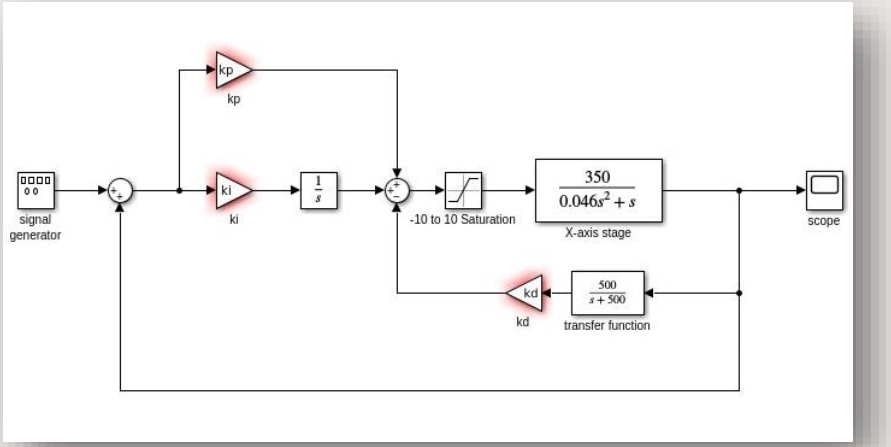

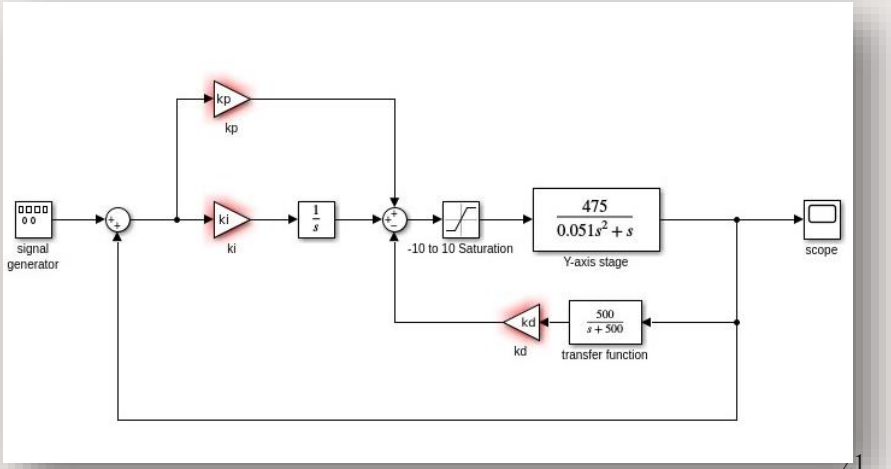

System identification, PID and Lead Compensator Design for XY stage

PID Controller Design

The PID controller designed is carried out using the MATLAB toolbox rltool. The PID parameters k_p , k_i, and k_d are tuned to achieve a step response for each plant of the stage to display a 20% overshoot and a rise time of 0.025 seconds. However, it is noted that higher percent overshoot for this design disappears when smooth trajectories are commanded to the plants instead of step inputs.

The picture on the top right shows The design control architecture chosen in MATLAB rltool toolbox is illustrated in the top right picture. Here, C1 represents the error path of the controller $\mathrm{k}_p + \mathrm{k}_i * \frac{1}{s}$ and C2 is the feedback path representing $\frac{\mathrm{k}_d * 500 * s}{s+500}$.

To conduct this design, an initial derivative gain value k_d=0.006 is selected. This value is iteratively adjusted until the desired percent overshoot and rise time criteria are met. Subsequently, the step response of the x-axis plant, as shown in the bottom right pictures, the picture, displays a 20% overshoot and a rise time of 0.253 s. These two parameters yield the following PID controller gain values for the x-axis plant : $\mathrm{k}_p = 0.7$, $\mathrm{k}_i = 3.13$ and $\mathrm{k}_d = 0.65$.

Similarly, performing the same procedure on the y-axis plant results in the following PID controller gain parameters: $\mathrm{k}_p = 1$, $\mathrm{k}_i = 2.2$ and $\mathrm{k}_d = 0.45$.

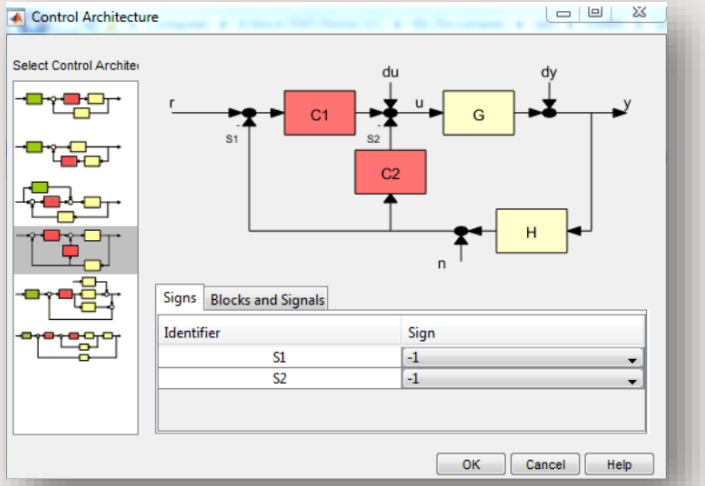

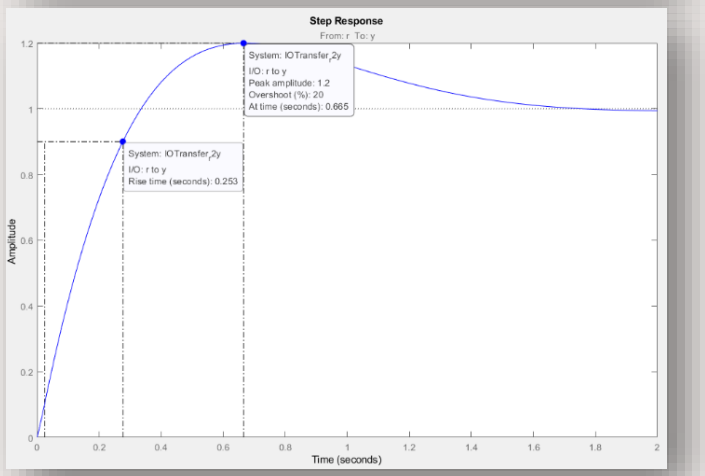

System identification, PID and Lead Compensator Design for XY stage

PID Controller with trajectory following implementation in Simulink

As previously discussed, the purpose of this project is to control the XY stage to follow a desired trajectory. In the previous slides, the plant transfer functions of each axis of the XY stage were identified using a closed-loop feedback and PID controllers were designed using MATLAB toolbox rltool. In this slide, the PID controller is implemented in Simulink to drive the physical plant.

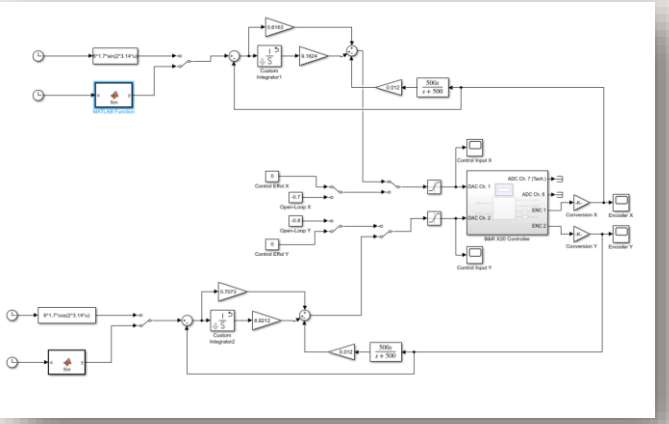

The top right picture illustrates the Simulink block diagram used to drive the system. This block diagram consists of six main components : an open-loop system, a B&R X20 controller, two saturation blocks, two closed-loop feedback system incorporating the designed PID controllers, two clocks , and two MATLAB function blocks.

The open-loop system centers the stage at coordinate (0,0) before starting to follow the desired trajectory. The B&R X20 controller acts as an interface between the closed-loop feedback system and the physical XY stage plant. Indeed, it converts the Digital signal output from the closed-loop to Analog signal that is used to generate motion on the XY stage.

To Generate the intended circular trajectory, the step input blocks to the closed-loop feedback system are replaced by the clock and the MATLAB function blocks. The clock block generates times in second, which serves as inputs to the function blocks. These blocks which generate the following signal for the X-axis and Y-axis of the stage, respectively.

$$x(t)= 10.2*\sin(2\pi * t)$$

$$y(t)= 10.2*\cos(2\pi * t)$$

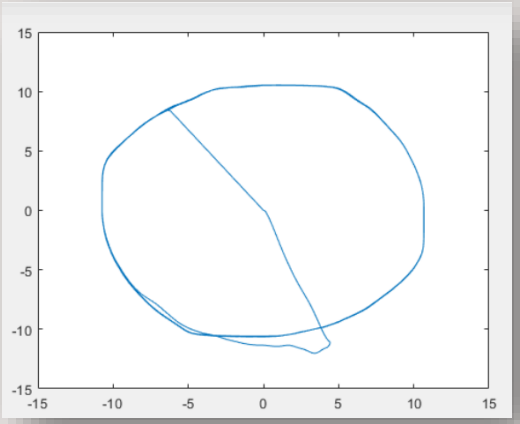

Driving the XY stage with these two input signals generates a circular trajectory motion of the XY stage. The bottom left image depicts a plot of such a circular trajectory obtained from the actual motion of the XY stage. The initial jump observed in the motion of the XY trajectory reflects the 20% overshoot design requirement. Furthermore, the benefit of using a PID controller is reflected in plot of the trajectory as the latter showcases stability of the XY stage, accurate tracking of the reference signal and the damping of the initial overshoot over time.

System identification, PID and Lead Compensator Design for XY stage

Lead Compensator Design

In the previous slide, system identification of the XY stage was performed, and a PID controller was designed according to system overshoot and rise time specifications to ensure the moving stage follows a circular trajectory. However, discrepancies between the mathematical model of the stage and the actual plant may cause the stage to become unstable upon the implementation of the controller. Hence, it is imperative to consider robustness when designing a controller for a plant. Robustness is expressed through phase and gain margin specifications.

The PID controller that was previously designed may not meet phase and gain margin specifications as it adds 0° phase to the plant. Two controllers that help meet robustness specifications are lead and lag controllers.

For this XY stage, two lead controller, one for each axis of the stage, are to be designed to ensure that the moving stage not only follows a circular trajectory but also maintain robustness. The following systems specification are chosen for designing these controllers: the compensated system need to have a phase margin $\Phi_{dm} = 60°$ and a gain margin $\mathrm{G}_{dm} = 20\ \mathrm{dB}$. Besides, since the plant of each axis is a type 1 system, it has zero position steady state error; hence, a steady state velocity error =$1/k_v$ is set. k_v is chosen to be 100 to mitigate frictional effects in tracking the steady state velocity error.

System identification, PID and Lead Compensator Design for XY stage

Lead Controller Design for the stage X-axis

A lead controller has the following mathematical form $C_{lead} = k_{lead} * \frac{Ts+1}{\alpha Ts+1}$. The parameters k_{lead} , T, and α of the controller can be determined using the phase margin, the gain margin, and the steady state velocity error specifications.

- Determining k_{lead} parameter

$k_{lead}=\frac{K_v}{K_{sys}} = \frac{100}{350} = 0.286$

- Determining T and α parameters

To calculate these two parameters, the bode diagram of the open-loop system $k_{lead}{}^{*}\ G_x$ is constructed using MATLAB. From, the bode diagram, the phase margin Φ_m, gain margin G_m, gain crossover frequency ω_g, and the phase crossover frequency ω_Φ of the uncompensated system can determined. The top right image shows such a bode diagram and indicates that the uncompensated system has Φ_m =26.19°, G_m= infinite, ω_g=infinite, and ω_Φ =44.1 rad/s. The uncompensated system already meets the gain margin design specification but not the phase margin specification. Indeed, the uncompensated system needs an additional phase Φ_{cm} to meet the phase margin designed specification . Φ_{cm}= Φ_{dm}- Φ_m +10°= 65°-26.19°+10°= 48.81°. Φ_{cm} is chosen to be the phase added by lead controller meet the design specification. From Φ_{cm}, $\alpha = 0.1819$ is obtained using the equation $\alpha=\frac{1-\sin(\Phi_{cm})}{1+\sin(\Phi_{cm})}$.

To leverage the maximum capability of the compensator, the maximum phase contribution frequency, ω_m, of the lead compensator is set to be the new gain cross-over frequency of the of the open-loop system $C_{lead}{}^{*}\ G_x$. Hence, setting ω_m as the new gain cross-over frequency yields $20*\log_{20} * [C_{lead}(j*\ \omega_m\ )*G(j*\ \omega_m\ )]=0$. Solving this equation yields T=0.046

Therefore, the following lead compensator was designed for the X-axis: $C_{lead} = 0.286 * \frac{0.046*s+1}{0.0083s+1}$. The bottom-right picture shows the bode diagram of the compensated system. The system effectively meets the desired phase and gain margin specifications.

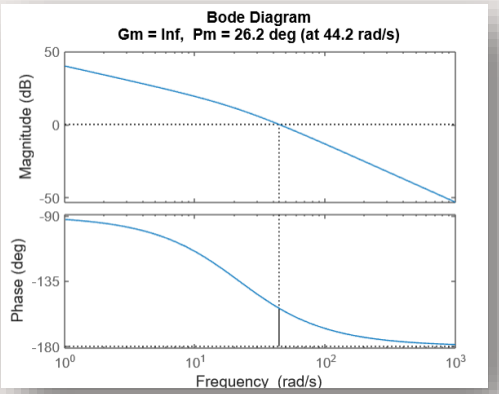

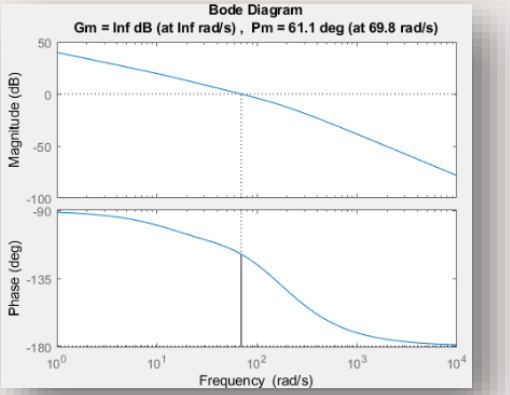

System identification, PID and Lead Compensator Design for XY stage

Lead Controller Design for the stage Y-axis

The lead compensator design for the Y-axis is done with MATLAB's SISOTOOL. The lead controller for the Y-axis has the form $C_{lead} = k_{lead} * \frac{Ts+1}{\alpha Ts+1}$. k_{lead} is determined using the static velocity error k_v and the constant gain of the plant k_{sys}. $k_{lead} = k_{lead} = \frac{K_v}{K_{sys}} = \frac{100}{475} = 0.211$.

To find the parameters T and α, SISOTOOL is applied to $k_{lead} * G_y$. SISOTOOL yields the root-locus plot, the bode plot, and the unit step response of $k_{lead} * G_y$. In SISOTOOL, the controller C_{lead} for the Y-axis is initially set as $\frac{s+1}{s+1}$ and the open-loop poles and zeros of

$C_{lead} * G_y$ are tuned on the root-locus plot until the gain and phase margin specifications are met. The top right picture shows the bode diagram, root-locus, step response of $C_{lead} * G_y$ with poles and zeros tuned to have $G_m = \text{infinite}$ and Φ_m=65°. From the phase and margin and gain cross-over frequency, the parameters T and α are obtained as follow: T= 1 and α =0.05 .

Therefore, the lead compensator for the Y-axis is C_{lead}=0.21* $\frac{s+1}{0.05s+1}$. The bottom right image shows the Simulink block diagram ,encompassing the designed lead controllers, that is used to drive the physical plant.